Chemical Engineering Journal 428 (2022) 131173

Contents lists available at ScienceDirect

Chemical Engineering Journal

journal homepage: www.elsevier.com/locate/cej

# Luteolin-based epoxy resin with exceptional heat resistance, mechanical and flame retardant properties

Tian-Yu Gao [1], Fen-Dou Wang [1], Yu Xu, Chun-Xiang Wei, San-E Zhu, Wei Yang [*], Hong-Dian Lu [*]

*School of Energy, Materials and Chemical Engineering, Hefei University, 99 Jinxiu Avenue, Hefei, Anhui 230601, PR China*

ARTICLE INFO

*Keywords:*
Luteolin
Epoxy resin
Heat resistance
Mechanical properties
Flame retardant

ABSTRACT

Recently, tremendous attentions have been paid to the fabrication of bio-based intrinsic fire-retarded epoxy resins with outstanding thermal and mechanical properties from renewable resources. Herein, the bio-based epoxy monomer of diglycidyl ether luteolin (DGEL) was synthesized via one-step method from sustainable luteolin. The biocompatible epoxy resin was manufactured via the curing reaction between DGEL and 4, 4′-diaminodiphenyl sulfone (DDS). DGEL/DDS showed higher glass transition temperature ($T_g$) (314.4 °C) than diglycidyl ether bisphenol A (DGEBA)/DDS (217.4 °C), demonstrating the distinguished heat resistance. Tensile testing results exhibited that DGEL/DDS possessed superior tensile strength (69.2 MPa) compared to DGEBA/DDS (57.2 MPa). Thermogravimetric analysis (TGA) illustrated that the char yield of DGEL/DDS was 44.0 wt%, much higher than that of DGEBA/DDS (11.6 wt%). In addition, DGEL/DDS passed the V-0 rating in UL-94 tests with a high limiting oxygen index (LOI) (32.5%) as well as extremely low peak heat release rate (107.5 W/g) indicating the excellent flame retardant properties. Smoke density testing results showed that the peak density of smoke for DGEL/DDS was 304.7, much lower than that for DGEBA/DDS (660.7), indicating the remarkable reduction of toxicity hazards. This work provides a facile approach for the preparation of bio-based epoxy resins with outstanding overall properties that show promising applications in high heat resistance and flame retardant fields.

## 1. Introduction

Epoxy resins are three-dimensional (3D) cross-linked thermosetting materials, which have been widely used in coatings, electronic materials, adhesives, aerospace and fiber reinforced composite substrates due to their excellent mechanical properties, high bonding strength, good heat resistance and low dielectric constants [1]. They are commonly manufactured via the cross-linking reaction between monomers and curing agents. Nevertheless, most currently used epoxy resins in the market are petroleum-based chemicals which are industrially produced based on bisphenol A (BPA) [2]. It is a hazardous compound that could affect our immune, brain and reproduction systems, leading to the prohibition of utilization in food packaging, baby bottles and other industries in European and American countries [3–5]. Moreover, the gradual depletion of fossil resources and environmental protection regulations severely limit the development of petroleum-based epoxy resins, resulting in the increasing demand on bio-based epoxy resins from renewable resources [6,7].

Nowadays, various biomass corps and plants are chosen as raw materials to fabricate thermosetting epoxy resins, including vegetable oil [8,9], lignin [10–12], itaconic acid [13,14], cardanol [15–17], gallic acid [18], eugenol [19,20], etc. To achieve outstanding flame retardant, mechanical and other properties in particular cases, many efforts have been devoted to the selection and design of epoxy monomer from bio-based compounds. For example, Tao et al. [21] synthesized a series of high-performance epoxy resins from protocatechuic acid, which showed enhanced thermal properties and mechanical properties ($T_g$ = 157 °C, tensile strength = 65 MPa) compared to commercial BPA-based epoxy resins. Wang et al. [22] reported several bio-based epoxy resins synthesized from eugenol that exhibited excellent flame retardant and mechanical properties, whereas the glass transition temperature ($T_g$) was decreased undesirably. The $T_g$ of epoxy resins, representing the heat resistance of materials, can be improved via the introduction of rigid aromatic ring to monomer from bio-based ingredients, such as vanillin and magnolol [23,24]. Xie et al. [25] used protocatechualdehyde to produce a Schiff-based epoxy resin with good fire-safety and mechanical

* Corresponding authors.
*E-mail addresses:* yangwei@hfuu.edu.cn (W. Yang), luhdo@hfuu.edu.cn (H.-D. Lu).
[1] Tian-Yu Gao and Fen-Dou Wang contributed equally to this work (co-first author).

https://doi.org/10.1016/j.cej.2021.131173
Received 21 March 2021; Received in revised form 18 June 2021; Accepted 2 July 2021
Available online 7 July 2021
1385-8947/

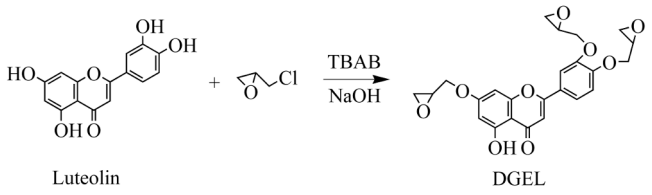


**Scheme 1.** Schematic synthesis route of DGEL.

properties (LOI = 40.5%, tensile modulus = 6.21 GPa). Nevertheless, the improvement of $T_g$ was limited. Therefore, it is still an enormous challenge to prepare bio-based epoxy resins with superior heat resistance and other enhanced properties by means of facile synthesis routes.

Similar to commercial BPA-based epoxy resins, the vast majority of biomass derived epoxy resins are flammable with the release of numerous smoke and toxic gases during combustion. Hence, the design and preparation of bio-based epoxy resins with high flame retardancy is one of the most concerned research topics. The effective approach to reduce the flammability of epoxy resins is to introduce flame retardant elements to the monomers and curing agents, such as halogen, silicon, phosphorous, or the mixed elements [16,26–29]. Unfortunately, halogen-containing flame retardants were proved to be harmful to the environment and human health [28–30]. The incorporation of halogen-free elements (P or Si) into epoxy resins can remarkably improve the flame retardant properties, whereas mechanical properties are reduced [31,32]. In consequence, the development of intrinsic flame retardant bio-based epoxy resins endowed with higher $T_g$ and sufficient mechanical properties is of great importance.

Luteolin is a kind of natural isoflavone compounds derived from various plants, including onion leaves, celery, green pepper and chamomile flower [33]. In the previous work, 4, 4′-bishydroxydeoxybenzoin (BHDB), similar to isoflavones, was utilized as raw materials to prepare epoxy resins, which showed outstanding flame retardant properties owing to the deoxybenzoin structure [34–37]. In this work, a novel fully bio-based epoxy monomer of diglycidyl ether luteolin (DGEL) was synthesized by one step method (see Scheme 1). DGEL was then cured with 4, 4′-diaminodiphenyl sulfone (DDS) to fabricate bio-based epoxy resin. The curing behaviors, thermal stability, heat resistance, mechanical and flame retardant properties of the cured resins were studied. In addition, the overall properties of DGEL/DDS were evaluated in comparison with commercial BPA-based epoxy resin.

## 2. Experimental

### 2.1. Materials

Luteolin (98%) was purchased from YuNing Biotechnology Co., Ltd., China. Epichlorohydrin (ECH), tetrabutylammonium bromide (TBAB, 99%) and 4, 4′-diaminodiphenyl sulfone (DDS, 97%) were obtained from Aladdin Reagent Co., Ltd., China. Sodium hydroxide (NaOH, ≥ 96%), dichloromethane (≥99.5%), ethyl acetate (≥99.5%), anhydrous magnesium sulfate (≥98%) were provided by Sinopharm Chemical Reagent Co., Ltd., China. Epoxy monomers, DGEBA (epoxy equivalent = 210–230 g/mol) were obtained from Nantong Xingchen Synthetic Materials Co., Ltd. All chemicals and solvents were used directly without further purification.

### 2.2. Synthesis of diglycidyl ether luteolin (DGEL)

Luteolin (20.7 g, 72.3 mmol), epichlorohydrin (ECH) (100.3 g, 1084 mmol) and tetrabutylammonium bromide (TBAB) (3.6 g, 3 wt% of the mixture) was added to the three-necked round-bottomed flask equipped with a reflux condenser and a magnetic stirrer. The mixture was stirred at 105 °C for 3 h. Subsequently, the reaction mixture was cooled to room temperature. The 40% w/w sodium hydroxide solution (28.9 g, 722.5 mmol of NaOH) was added dropwise to the reaction system in 1 h with constant stirring for another 5 h at room temperature. After the mixture was dissolved in dichloromethane and washed with deionized water. Then the organic layer was dried using anhydrous magnesium sulfate for 12 h. After filtration, the dried organic layer was concentrated in rotary evaporator to remove the dichloromethane and excess epichlorohydrin. The obtained yellow solid product was dried in a vacuum oven at 75 °C for 12 h. The pure product was purified by silica gel chromatography (dichloromethane/ethyl acetate: 15/1) (22.3% yield). $^1$H NMR (400 MHz, $CDCl_3$, ppm): $\delta$ = 12.77 (s, 1H), 7.51 (m, 1H), 7.45 (d, H), 7.02 (d, 1H), 6.57 (s, 1H), 6.51 (d, 1H), 6.36 (d, 1H), 4.44–4.38 (m, 2H), 4.35–4.32 (m, 1H), 4.09–4.03 (m, 2H), 4.02–3.97 (m, 1H), 3.45–3.37 (m, 3H), 2.97–2.94 (t, 3H), 2.84–2.78 (t, 3H). $^{13}$C NMR (101 MHz, $CDCl_3$, ppm): $\delta$ = 182.31, 164.16, 163.60, 162.14, 157.52, 151.84, 149.63, 124.44, 120.88, 113.77, 112.50, 105.80, 104.81, 98.54, 93.21, 70.61, 69.91, 69.22, 50.22, 50.04, 49.74, 44.66, 44.62, 44.58.

### 2.3. Preparation of DGEL and DGEBA epoxy resins

Epoxy resins (DGEBA or DGEL) and curing agent (DDS) in the stoichiometric ratio (molar ratio of N–H group/epoxy group is 1:1) were melted at 200 °C (or 190 °C) respectively, and then blended and stirred to obtain a uniform mixture. It was quickly poured into a preheated Teflon mold at 200 °C, and the curing reaction was performed in an air-circulating oven at 180, 200 and 220 °C for 2 h at each temperature. The DGEBA was cured with DDS under the same conditions.

### 2.4. Characterizations

The chemical structure of epoxy monomer was characterized by $^1$H NMR and $^{13}$C NMR spectra recorded on a 400 MHz AVANCE III Bruker NMR spectrometer, using deuterated chloroform ($CDCl_3$) as the solvent and tetramethysilane (TMS) as an internal standard. The epoxy monomer was also characterized by using Fourier transform infrared (FTIR) spectrometer (Nicolet iS 50+, Thermo Fisher Scientific Inc., USA).

The curing behaviors were analyzed via differential scanning calorimetry (DSC) (TA Q200). The mixture (the range of 5–10 mg) was placed in an aluminum crucible and heated from 25 to 300 °C or 350 °C at rates of 5, 10, 15 and 20 °C/min in a high-purity nitrogen atmosphere. The degree of hardening was measured by using FTIR spectrometer (Nicolet iS 50+, Thermo Fisher Scientific Inc., USA).

Thermogravimetric analysis (TGA) was carried out on a TA Instruments (TA Q500) under nitrogen and air conditions. The samples were heated from 50 to 700 °C with a heating rate of 20 °C/min.

Dynamic mechanical analysis (DMA) was performed on TA Instruments Q800 in air. The sample with the dimension of 10 × 6 × 2 $mm^3$ was tested at a heating rate of 3 °C/min and constant frequency of 1 Hz.

The mechanical properties of cured resins were assessed using a Universal Mechanical Testing Machine (China). The crosshead speed is 50 mm/min for tensile properties. An average of five individual determinations was obtained.

Thermal combustion properties were determined by microscale combustion calorimetry (MCC, Govmark) according to ASTM D 7309–07. 4–8 mg of each sample was heated at 1 °C/s from room temperature to 750 °C and held there for 30 s.

Smoke density tests were performed in a NBS chamber (VOUCH 5920, Suzhou Vouch Testing Technology Co. Ltd., China) according to ISO 5659. The sample with the dimension of 75 × 75 × 3 $mm^3$ was tested in the chamber with a heat flux of 25 $kW/m^2$.

Limiting oxygen index (LOI) was determined by an HC-2 Oxygen Index instrument (Jiangning Analytical Instrument Co. Ltd., China) according to ASTM D2863-2008. The sample size in the test was 100 × 6.5 × 3 $mm^3$.

UL-94 vertical burning tests were performed on a following the procedure described in ANSI/UL 94–2010 via a CFZ-2-type instrument

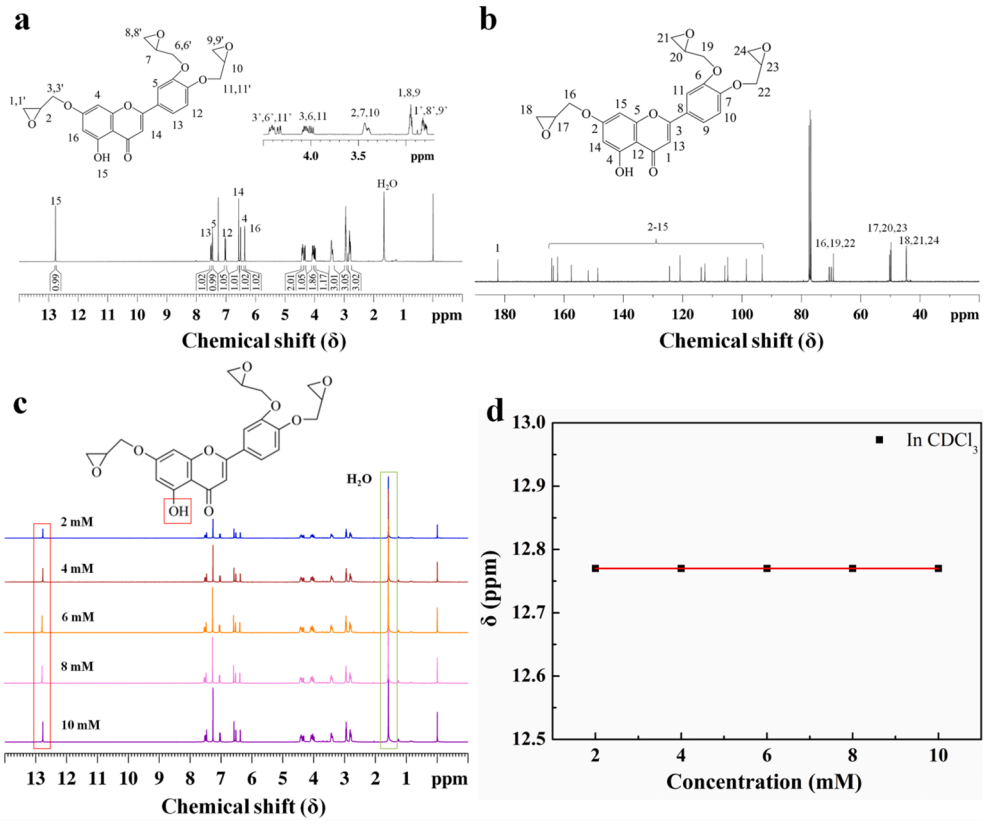


**Fig. 1.** (a) $^{1}$H NMR spectra ($CDCl_3$) of DGEL; (b) $^{13}$C NMR spectra ($CDCl_3$) of DGEL; (c) and (d) Variation of the chemical shift of the Ar–OH in DGEL as a function of the solvent concentration at 25 °C.

(Jiangning Analysis Instrument Company, China). The samples size was 130 × 13 × 3 mm$^3$.

The morphology of char residues after LOI tests was observed using Hitachi SU8010 SEM (Japan) under high vacuum with a voltage of 10 kV. Prior to SEM observations, a conductive gold layer was coated on the char residues.

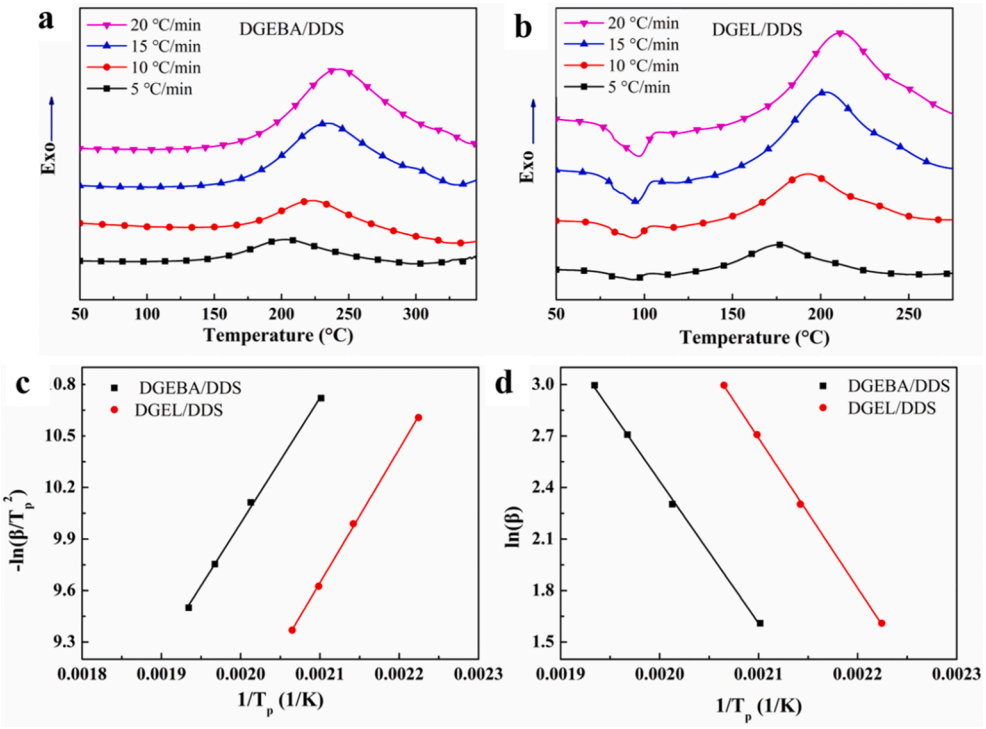


**Fig. 2.** Exothermic curves from DSC of DGEBA/DDS (a) and DGEL/DDS (b) curing systems; Linear of $-\ln(\beta/T_P^2)$ versus $1/T_p$ of DGEL/DDS and DGEBA/DDS curing systems based on Kissinger's method (c); Linear of $\ln(\beta)$ versus $1/T_p$ of DGEL/DDS and DGEBA/DDS curing systems based on Ozawa's method (d).

**Table 1**
The cure characteristics and related data for DGEBA/DDS and DGEL/DDS.

| Samples | Heating rate (°C/min) | $T_{onset}$ (°C) | $T_p$ (°C) | $T_{endset}$ (°C) | ΔT (°C) | $\Delta H_\infty$ (J/g) | CI |
|---|---|---|---|---|---|---|---|
| DGEL/DDS | 5 | 137.5 | 176.4 | 233.0 | 95.5 | 392.4 | 0.98 |
| | 10 | 151.0 | 193.7 | 255.1 | 104.1 | 355.0 | 1.18 |
| | 15 | 159.2 | 203.4 | 267.0 | 107.8 | 411.8 | 1.19 |
| | 20 | 166.4 | 211.1 | 276.6 | 110.2 | 351.0 | 1.08 |
| DGEBA/DDS | 5 | 152.0 | 202.7 | 268.3 | 116.3 | 334.5 | 1.00 |
| | 10 | 171.4 | 223.7 | 291.3 | 119.9 | 263.0 | 1.00 |
| | 15 | 176.7 | 235.1 | 323.4 | 146.7 | 329.3 | 1.00 |
| | 20 | 183.0 | 243.8 | 334.7 | 151.7 | 311.7 | 1.00 |

Laser Raman spectroscopy was carried out by Laser-Confocal Micro Raman Spectrometer of Thermo Fisher (DXR, USA) in the wavenumber range of 500–2000 $cm^{-1}$.

TGA-FTIR spectra were recorded on a TA Instruments (TA Q50) under nitrogen with a Thermo Fisher FTIR. The temperature of transferring line between TGA and FTIR was determined to be 200 °C. 5–10 mg specimen was heated from 50 to 700 °C under a nitrogen atmosphere at the heating rate of 20 °C/min. FTIR spectra were collected every 40 s during the whole testing process.

Pyrolysis-gas chromatography/mass spectrometry (Py-GC/MS) was performed on an EGA/PY3030D furnace pyrolyzer (Frontier Japan) coupled with a Thermo Fisher TRACE1310/Thermo ISQLT GC/MS. The cracker temperature was set at 500 °C and held on 20 s under helium atmosphere.

## 3. Results and discussion

### 3.1. Characterization of DGEL

The chemical structure of DGEL was verified using $^1$H NMR (Fig. 1a), $^{13}$C NMR (Fig. 1b) and FTIR (Fig. S1). The $^1$H NMR and $^{13}$C NMR spectra clearly show that the chemical shift and integral area of all the peaks correspond well with the predicted chemical structure. Unlike the other hydroxyls, the phenolic hydroxyl group close to carbonyl group in DGEL was not involved in the reaction. It is attributed to the formation of strong intramolecular hydrogen bond between —OH and oxygen atom on the carbonyl group that reduces the reactivity of phenolic hydroxyl group [35,38]. The chemical shift of the phenolic hydroxyl group without the intermolecular force will change with the concentration and temperature. Conversely, the intramolecular hydrogen bond can lead to the invariable chemical shift whatever the concentration or temperature changes. As illustrated in Fig. 1(c, d), the chemical shift of Ar-OH in DGEL remains stable despite the changed concentration of aprotic solution. It means that a strong intramolecular hydrogen bond is generated between Ar-OH and carbonyl group leading to the remarkably reduced reactivity. In the FTIR spectrum of DGEL, the peak at 3200–3400 $cm^{-1}$ corresponding to —OH vibration almost disappears. The characteristic absorption peak of epoxy groups occurs at 910 $cm^{-1}$ indicating the formation of epoxy group. Therefore, it can be concluded that the characterization results strongly support the predicted chemical structure of DGEL.

### 3.2. Curing behaviors

The curing behavior of DEGL/DDS and DGEBA/DDS systems was studied by non-isothermal curing kinetics and depicted in Fig. 2. For both DGEL/DDS and DGEBA/DDS system, the DSC heating curves present an exothermic peak, which corresponds to the ring-opening reaction between epoxy resin and amino group. In addition, there are two overlapping endothermic peaks in the DGEL/DDS system related to the complex melting process of DGEL and DDS. The curing exothermic peak temperature of DGEL/DDS is lower than that of DGEBA/DDS. The peak temperature in the non-isothermal DSC curves can be used as an index to evaluate the curing reactivity of epoxy resins. The cure index (CI) is a simple criterion to investigate the qualitative evaluation of cross-linking situation [39]. The CI equation was elucidated in Eq. (S1) and the values were listed in Table 1. Compared to DGEBA/DDS, the higher CI for DGEL/DDS indicates that the curing system is attributed to "excellent cure" that is mainly controlled by chemical kinetics in the early stage of curing. It has strong activity under the condition of providing sufficient energy, leading to the curing in a narrow temperature range [40]. The early curing reaction results in the premature formation of the curing system that limits the interaction between the polymer chain and the curing agent.

**Table 2**
Activation energies of DGEL/DDS and DGEBA/DDS.

| Samples | $E_a$ (kJ/mol) | | $R^2$ | |
|---|---|---|---|---|
| | Kissinger | Ozawa | Kissinger | Ozawa |
| DGEL/DDS | 64.8 | 69.0 | 0.99939 | 0.99947 |
| DGEBA/DDS | 60.7 | 65.5 | 0.99803 | 0.99835 |

The apparent activation energy of curing reaction determines the kinetics of curing reaction of epoxy resin system. The activation energy ($E_a$) of the two systems was calculated via Kissinger's equation (1) and Ozawa's methods (2) [41].

$$-\ln\left(\frac{\beta}{T_p^2}\right) = -\ln\left(\frac{AR}{E_a}\right) + \frac{E_a}{RT_p} \quad (1)$$

$$\ln\beta = -1.052 \times \frac{E_a}{RT_p} + \ln\left(\frac{AE_a}{R}\right) - \ln F(x) - 5.331 \quad (2)$$

where q is the heating rate, $T_p$ is the exothermic peak temperature, $E_a$ is the activation energy, R is the gas constant and A is the pre-exponential factor. The apparent activation energy values can be calculated from the slope of the linear fitting plot. The related data were calculated and presented in Fig. 2 (c and d) and Table 2. It is observed that $E_a$ of DGEL/DDS (64.8 kJ/mol by Eq. (1) and 69.0 kJ/mol by Eq. (2)) is slightly higher than that of DGEBA/DDS (60.7 kJ/mol by Eq. (1) and 65.5 kJ/mol by Eq. (2)). This can be attributed to the fact that DGEL possesses more epoxy groups. The curing reaction will be accelerated once the activation energy is achieved.

According to the test results of DSC, the curing conditions of DGEL/DDS and DGEBA/DDS were set as 180 °C/2h, 200 °C/2h and 220 °C/2h. Fig. S2 shows the FTIR spectra of epoxy monomer (DGEL) and cured resin (DGEL/DDS). From the FTIR spectrum of DGEL, it is clearly observed that the characteristic absorption peak located at 910 $cm^{-1}$ is attributed to the vibration of epoxy groups. The peaks at 860 and 1660 $cm^{-1}$ are ascribed to the vibration of C═C in benzopyrone ring. Compared to DGEL, the absorption peaks corresponding to epoxy groups and C═C in DGEL/DDS disappear after curing reaction. It indicates that the epoxy groups are involved in the curing reaction with high degree of curing. In addition, the absence of C═C in DGEL/DDS implies the cross-linking reaction via C═C in the benzopyrone between different molecular chains [34,42] (see Fig. S3).

### 3.3. Thermal stability

The thermal stability of DGEL/DDS and DGEBA/DDS under $N_2$ and air conditions was studied by TGA (Fig. 3). As illustrated in Fig. 3 (a, b), the $T_{d5\%}$ (temperature at 5% weight loss) and $T_{d30\%}$ (temperature at 30% weight loss) of DGEL/DDS under $N_2$ condition are 379.0 °C and 414.7 °C, respectively, which are lower than those of DGEBA/DDS (393.3 °C and 420.2 °C). Moreover, $T_{max}$ (the temperature at the maximum degradation rate) of DGEL/DDS is lower than that of DGEBA/DDS (400.7 °C vs 429.0 °C). It is caused by the early decomposition of the benzopyrone ring in the DGEL/DDS cross-linking structure [35]. In

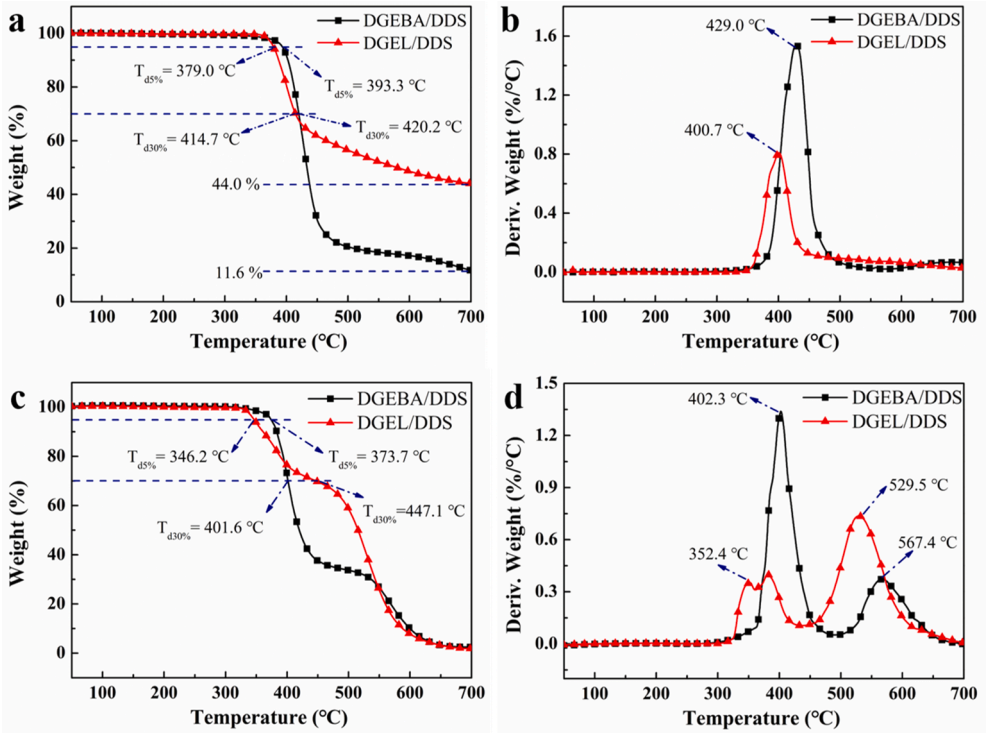


**Fig. 3.** TGA and DTG curves of DGEL/DDS and DGEBA/DDS in $N_2$ (a and b) and air (c and d).

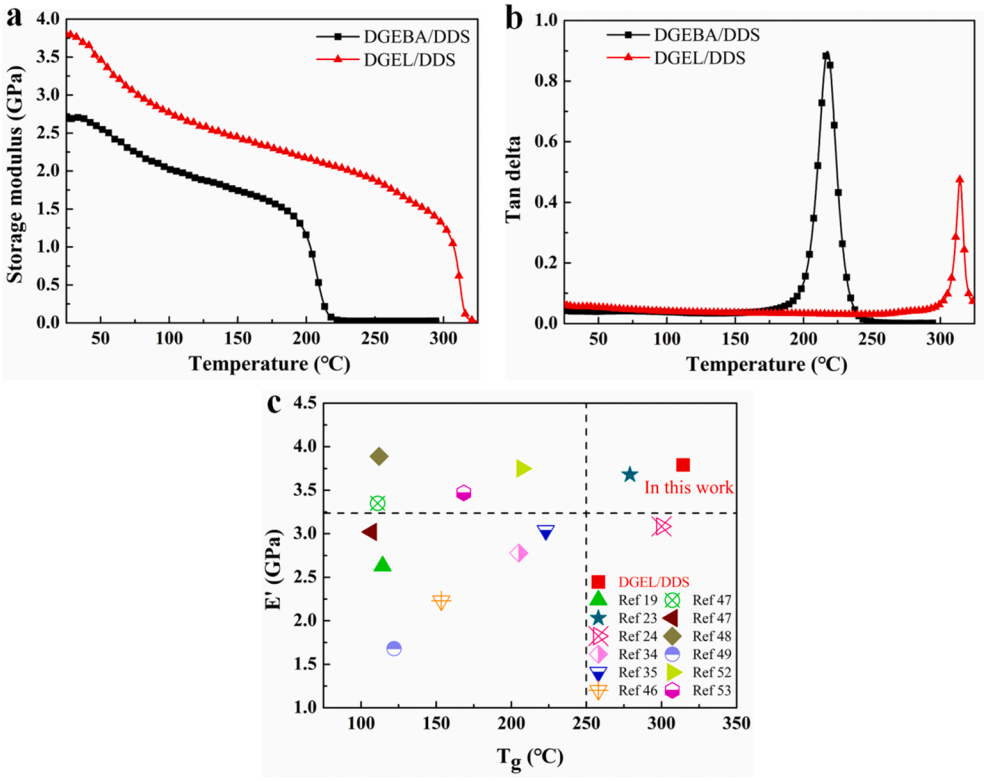


**Fig. 4.** Storage modulus (a) and tangent delta (b) versus temperature from DMA measurements for DGEL/DDS and DGEBA/DDS; (c) Comparison of $T_g$ and E′ for DGEL/DDS in this work with other bio-based epoxy resins reported in the literatures.

Fig. 3a, the residual yield of DGEL/DDS at 700 °C is 44.0 wt% which is approximatively 4 times as much as that of as DGEBA/DDS (11.6 wt%). To evaluate the carbonization ability of DGEL/DDS, the comparison with other reported results was conducted and summarized in Table S1. The char yield of DGEL/DDS (44.0 wt%) is higher than that of most bio-based epoxy resins, such as DGED/DDM (42.9 wt%) [34], DGEM/DDS (42.8 wt%) [23], VBE/DDM (40.8 wt%) [43], DEU-EP (38.0 wt%) [19], etc. It suggests that DGEL/DDS possesses a stronger carbonization ability

**Table 3**
E′ at different temperatures, $T_g$, $v_e$ and tensile properties for DGEL/DDS and DGEBA/DDS.

| Sample | E′ (GPa) at 30 °C | E′ (GPa) at 220 °C | $T_g$ (°C) | $v_e/10^3$ (mol/$m^3$) | Tensile strength (MPa) | Elongation at break (%) |
|---|---|---|---|---|---|---|
| DGEL/DDS | 3.79 | 2.07 | 314.4 | 1.5 | 69.2 ± 1.5 | 9.5 ± 1.2 |
| DGEBA/DDS | 2.69 | 0.05 | 217.4 | 2.2 | 57.2 ± 2.2 | 10.8 ± 0.6 |

that is beneficial to the fire resistance performance.

The thermal degradation behaviors of DGEL/DDS and DGEBA/DDS in air are different from that in nitrogen. The related results are exhibited in Fig. 3(c, d). Both DGEL/DDS and DGEBA/DDS show two thermal degradation stages under air condition. The $T_{max}$ values of DGEL/DDS in the two degradation stages are 352.4 °C and 529.5 °C, respectively, which are lower than those of DGEBA/DDS (402.3 °C and 567.4 °C). As shown in Fig. 3c, the char yield of DGEL/DDS at 500 °C is 58.6 wt%, which is much higher than that of DGEBA/DDS (33.7 wt%). From DTG curves (Fig. 3b and 3d), both the peaks of weight loss rate under nitrogen and air condition for DGEL/DDS are greatly lower than those for DGEBA/DDS. The high char yield and reduced weight loss rate of DGEL/DDS indicate that more organic ingredients are involved in the charring reaction leading to the reduction of gas volatiles. The excellent carbonization characteristics of DGEL/DDS will contribute to self-extinguishing of burning when exposed to high temperature or flame.

### 3.4. Dynamic mechanical properties

Dynamic mechanical behavior of cured bio-based epoxy thermosets was evaluated via DMA testing. Fig. 4 shows the storage modulus (E′) and tan delta as a function of temperature for DGEL/DDS and DGEBA/DDS. The related parameters, including E′, $T_g$ and cross-linking density ($v_e$), are summarized in Table 3. When the temperature is 30 °C, the E′ of DGEL/DDS is 3.79 GPa, which is 41% higher than that of DGEBA/DDS (2.69 GPa). Moreover, at 220 °C, the E′ of DGEL/DDS is 2.07 GPa, much higher than that of DGEBA/DDS (0.05 GPa). The largely improved storage modulus of DGEL/DDS is primarily attributed to the additional benzopyrone ring in DGEL leading to the enhancement of rigidity in the cured resin, which is in good agreement with the previous work [35]. In addition, the intermolecular cross-linking reaction via C═C in benzopyrone ring promotes the formation of highly cross-linked 3D network structure which further improves the stiffness [35] (Fig. S2 and S3).

Glass transition temperature (the temperature determined by the peak value of tan delta, $T_g$) is an important parameter to determine the heat resistance of polymers. From Fig. 4b, it is clearly observed that the $T_g$ of DGEL/DDS is much higher than that of DGEBA/DDS (314.4 °C versus 217.4 °C). Compared to DGEBA, the accessional benzopyrone rings in DGEL inducing the extra cross-linking between chains remarkably restrain the chain rotation which leads to the increased $T_g$. The extremely high $T_g$ can expand the application of epoxy resin in high heat resistance fields, especially aerospace ($T_g \geq 220$ °C) [44]. To evaluate the dynamic mechanical properties, storage modulus (E′) and glass transition temperature ($T_g$) for DGEL/DDS were compared with the reported results [10,18,19,21,23–25,34,35,43,45–54] (see Fig. 4c and Table S1). Astonishingly, the $T_g$ value of DGEL/DDS is the highest in all reported results with preferable E′ value which indicates the outstanding heat resistance and mechanically stable properties.

According to the rubbery elasticity theory [55], the $v_e$, representing the cross-linking density of thermosets, can be calculated from the following formula:

$$E' = 3v_eRT \quad (3)$$

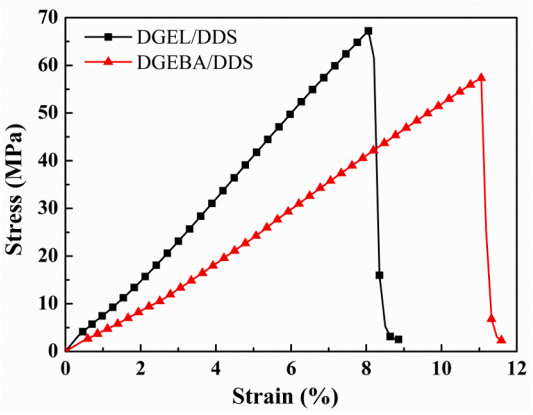


**Fig. 5.** The stress–strain curves of the cured DGEL/DDS and DGEBA/DDS from tensile tests.

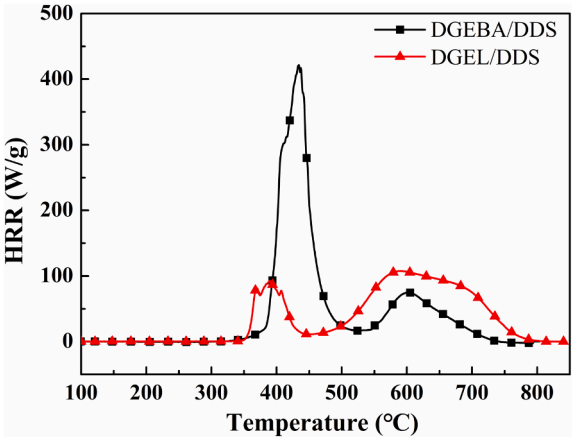


**Fig. 6.** HRR curves of DGEL/DDS and DGEBA/DDS from MCC tests.

where E′ is the storage modulus of the epoxy resins at T = ($T_g$ + 10) °C, R is the ideal gas constant, and T is the absolute temperature. Calculated $v_e$ of the cured epoxy resins are listed in Table 3. The $v_e$ of DGEL/DDS and DGEBA/DDS are 2.2 × $10^3$ mol/$m^3$ and 1.5 × $10^3$ mol/$m^3$, respectively. Although the cross-linking density of DGEL/DDS is lower than that of DGEBA/DDS, the higher $T_g$ of DGEL/DDS can be attributed to the higher rigidity of DGEL and the excellent 3D network that is generated during the curing reaction between DGEL with three epoxy groups and DDS.

### 3.5. Tensile properties

Mechanical performance is one of the most important properties of thermosetting epoxy resin. Tensile stress–strain curves of cured DGEL/DDS and DGEBA/DDS are shown in Fig. 5, and the corresponding data are listed in Table 3. The tensile strength of DGEL/DDS is 69.2 MPa, which is higher than that of DGEBA/DDS (57.2 MPa). The tensile strength of epoxy resins is dependent on the cross-linking density and molecular rigidity [24]. Owing to the lower cross-linking density of DGEL/DDS (see Table 3), the improved tensile strength is dominantly attributed to the higher rigidity of the system. The DMA results have demonstrated the significantly enhanced rigidity that endows DGEL/DDS with superior stiffness. It contributes to the improvement of tensile strength. However, the rigid structure restricts the mobility of network segments leading to the slightly reduced elongation at break (9.5%) in comparison with DGEBA/DDS (10.8%). These results indicate that DGEL/DDS possesses higher mechanical strength with acceptable degree of strain.

**Table 4**
MCC data for DGEL/DDS and DGEBA/DDS.

| Sample | HRC (J/gk) | PHRR (W/g) | THR (kJ/g) | $T_p$ (°C) | |
|---|---|---|---|---|---|
| | | | | $T_{p1}$ | $T_{p2}$ |
| DGEL/DDS | 101.0 | 107.5 | 24.3 | 390.1 | 589.8 |
| DGEBA/DDS | 399.1 | 421.9 | 29.1 | 434.4 | 602.3 |

### 3.6. Flame retardancy

The thermal combustion performance of DGEL/DDS and DGEBA/DDS in this study was analyzed by MCC, which can characterize the intrinsic/material combustion properties [56–58]. As demonstrated in Fig. 6, both the HRR curves for DGEL/DDS and DGEBA/DDS show two peaks, representing the two stages of degradation, which is consistent with the TGA curves (see Fig. 3). The $T_p$ values ($T_{p1}$ = 434.4 °C, $T_{p2}$ = 602.3 °C) of DGEBA/DDS are higher that of DGEL/DDS ($T_{p1}$ = 390.1 °C, $T_{p2}$ = 589.8 °C), resulting from the preferable thermal stability. However, DGEL/DDS shows much lower heat release capacity (HRC), peak heat release rate (PHRR) and total heat release rate (THR). Compared to DGEBA/DDS (399.1 J/gk, 421.9 W/g, 29.1 kJ/g), the HRC, PHRR and THR of DGEL/DDS (101.0 J/gk, 107.5 W/g, 24.3 kJ/g) are reduced by 74.7%, 74.5% and 16.5%, respectively (Table 4). The results indicate that the flammable gas products decomposed from DGEL/DDS are much less than that from DGEBA/DDS contributing to the improved flame retardant properties.

Flammable materials during combustion can generate tremendous amount of toxic smoke and soot. The smoke production behaviors of DGEL/DDS and DGEBA/DDS were evaluated by smoke density test [59,60]. The variation of smoke density with time is shown in the Fig. 7. As illustrated in Fig. 7a, the reduction of light transmittance for DGEL/DDS is earlier than that for DGEBA/DDS, resulting from the lower thermal stability of DGEL/DDS. The light transmittance of DGEL/DDS is 1.5% at 400 s, which is slightly higher than that of DGEBA/DDS (almost 0 at 400 s). It indicates that the smoke production of DGEL/DDS is reduced. In Fig. 7b, the smoke density of DGEBA/DDS reaches a peak value of 660.7 at 1013 s, while the peak of smoke density for DGEL/DDS is as low as 304.7. The reduction of 53.9% in smoke density indicates that the smoke production of DGEL/DDS is significantly reduced during the combustion process. In addition, the char yield of DGEL/DDS is 66.0 wt%, which is higher than that of DGEBA/DDS (50.5 wt%) (see Fig. S4). It further confirms that DGEL/DDS shows more significant carbonization ability that reduces the heat release and fuels emission leading to the reduction of smoke density.

UL-94 and LOI tests are effective methods to evaluate the combustion behaviors of polymers. A view of the epoxy resins during the UL-94 tests is shown in Fig. 8. DGEBA/DDS was burned drastically until the end of the test with serious dripping during the combustion process. DGEL/DDS can self-extinguish after the first and second ignition without any drips. When the flame was removed, the burning time was no more than

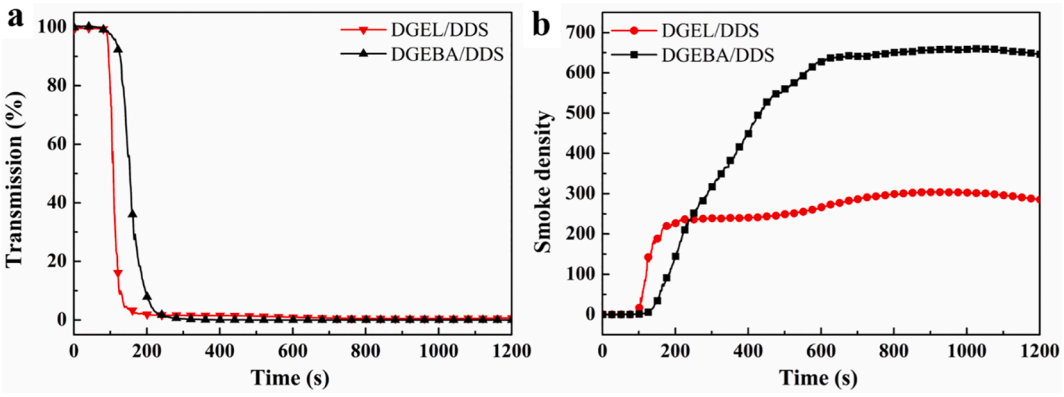


**Fig. 7.** Light transmission (a) and smoke density (b) curves for DGEL/DDS and DGEBA/DDS with a heat flux of 25 kW/m$^2$.

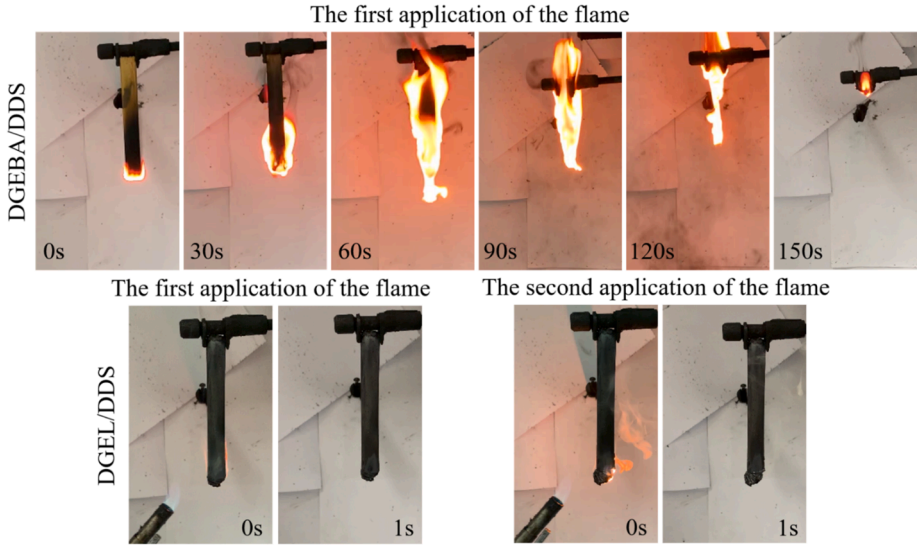


**Fig. 8.** Digital photos taken from the representative moments of UL-94 tests for DGEBA/DDS and DGEL/DDS.

**Table 5**
The LOI and UL-94 data of DGEL/DDS and DGEBA/DDS.

| Sample | LOI (%) | UL-94 | Flaming drips |
|---|---|---|---|
| DGEL/DDS | 32.5 ± 0.5 | V-0 | No |
| DGEBA/DDS | 27.0 ± 0.5 | NR | Yes |

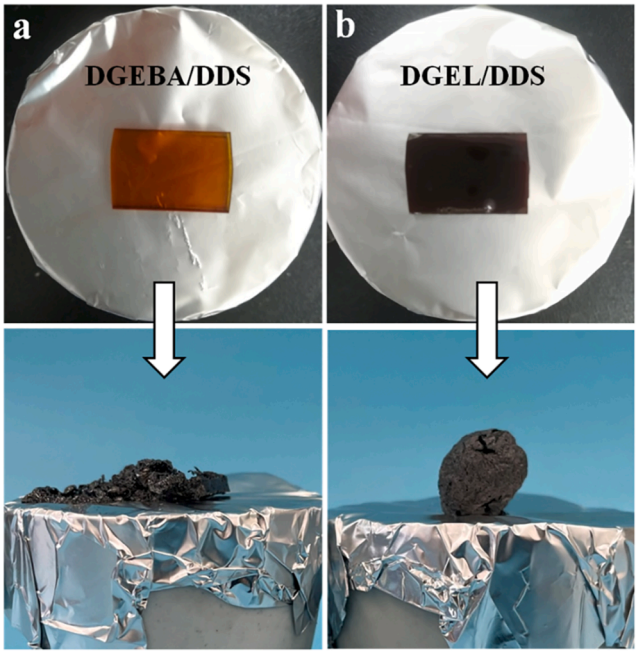


**Fig. 9.** Digital photos of (a) DGEBA/DDS and (b) DGEL/DDS before and after calcination at 500 °C in air.

1 s (see Fig. 8). It indicates that DGEL/DDS is nonflammable as well as passing the V-0 rating in UL-94 test (Table 5). In addition, the LOI of DGEL/DDS is 32.5%, higher than that of DGEBA/DDS (27.0%). These results demonstrate that DGEL/DDS possesses outstanding flame retardant properties.

Fig. 9 presents the morphology of epoxy resin before and after calcination. It is observed that after calcination of DGEBA/DDS, a small amount of char residues are left with a collapse and fragment appearance, indicating the sufficient burning in furnace. In contrast, DGEL/DDS forms effective expandable char residues, confirming the superior flame retardant properties. In addition, the height of the expansion char for DGEL/DDS is much higher than that for DGEBA/DDS. It suggests that the char residues for DGEL/DDS are mechanically stable, which is favorable for reducing the release of combustible gases and protecting the interior of the matrix.

### 3.7. Residue analysis

The char residues of DGEL/DDS and DGEBA/DDS after LOI tests were characterized by SEM and Raman spectroscopy. The char residues of DGEL/DDS are compact and smooth, which can effectively prevent the transfer of heat and flammable materials (Fig. 10a). However, the presence of tremendous amount of defects and holes on the char surface of DGEBA/DDS (Fig. 10b) can promote the rapid transfer of heat and combustible gases that accelerates the burning. As illustrated in Raman spectra (Fig. 10c and 10d), there are two obvious overlapping peaks at 1337 $cm^{-1}$ (D band) and 1572 $cm^{-1}$ (G band), which are attributed to amorphous and graphitized carbons [61,62], respectively. The degree of graphitization of carbon residues can be determined by the integral intensity ratio ($I_D/I_G$) of the two bands. Higher graphitization degree can be achieved with lower $I_D/I_G$ value [63]. In general, the char residues with higher graphitization degree have superior thermal oxidation resistance which contributes to the improvement of fire retarded properties of polymers [64,65]. The $I_D/I_G$ value of DGEL/DDS is lower than that of DGEBA/DDS, indicating that the graphitization degree of char residues is improved during combustion. It suggests that DGEL/DDS can form a more stable char layer with excellent thermal oxidation

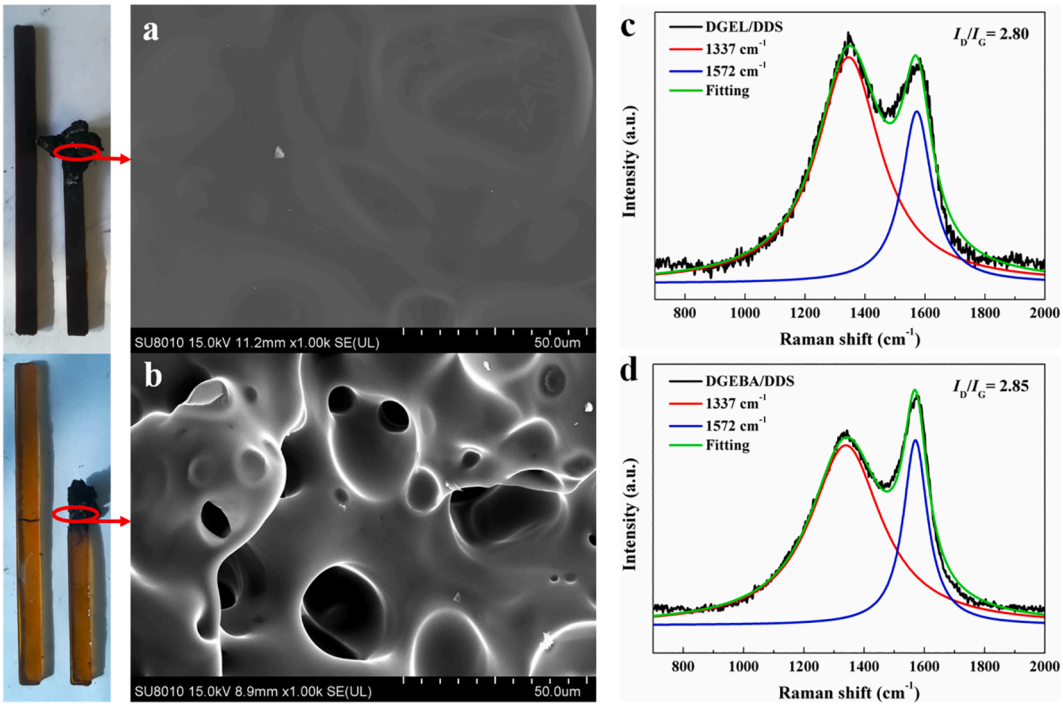


**Fig. 10.** Digital photographs before and after LOI tests and SEM images of char residues for DGEL/DDS (a) and DGEBA/DDS (b); Raman spectra of char residues for DGEL/DDS (c) and DGEBA/DDS (d).

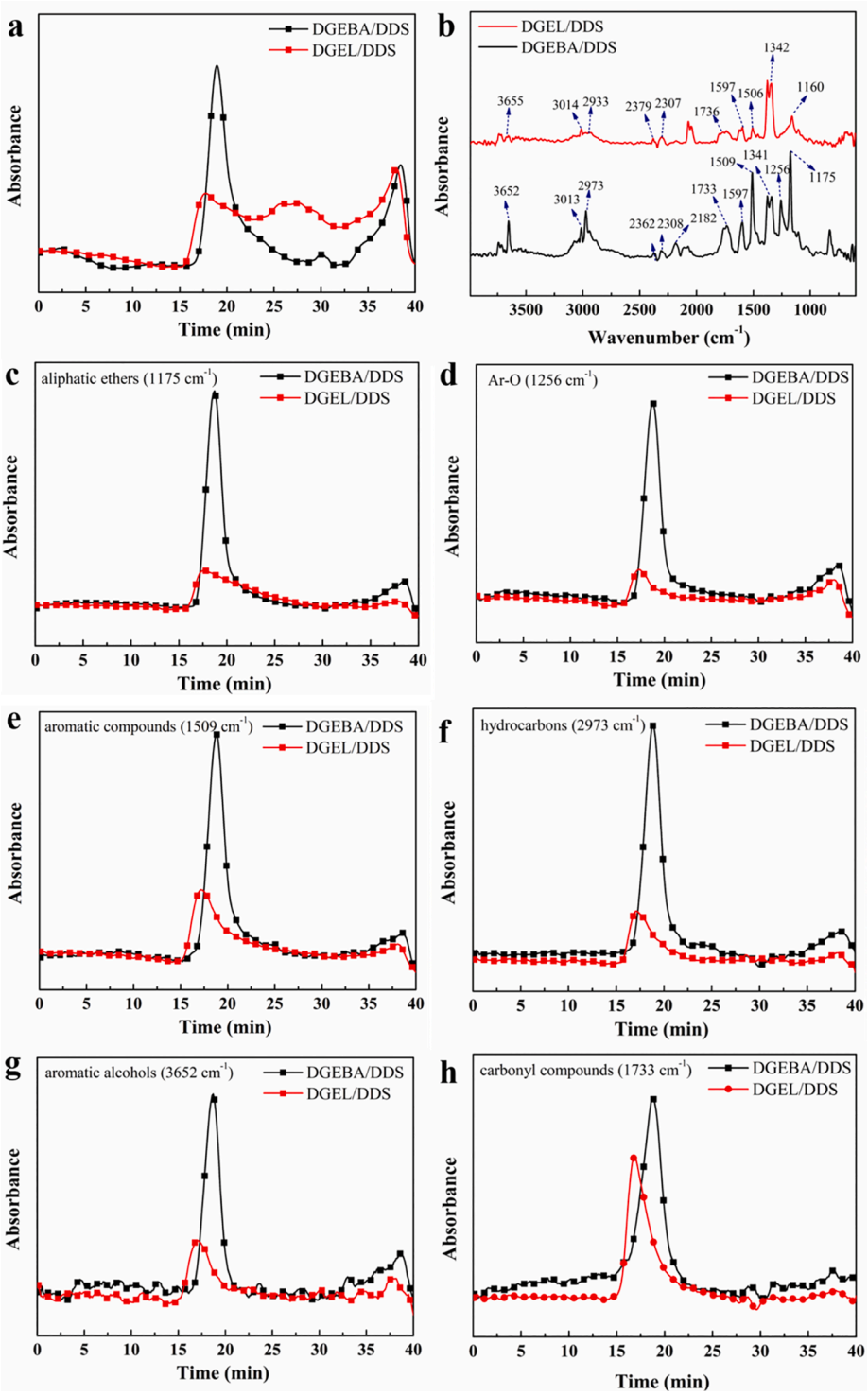


**Fig. 11.** Total absorptions spectra of the gaseous products for DGEL/DDS and DGEBA/DDS (a); the FTIR spectra of the pyrolysis products of the cured resins DGEL/DDS and DGEL/DDS at the maximum decomposition rate (b); aliphatic ethers (c); Ar-O (d); aromatic compounds (e); hydrocarbons (f); aromatic compounds (g); carbonyl compounds (h).

resistance to inhibit the emission of flammable gas products or free radicals, which leads to the notable enhancement of self-extinguish ability.

### 3.8. Flame retardant mechanism

To further study the flame retardant mechanism of DGEL/DDS, TGA-FTIR and Py-GC/MS were utilized to analyze the gaseous substances released during thermal decomposition (Fig. 11). As illustrated in Fig. 11a, the total gas products generated in the degradation process of DGEL/DDS are lower than that of DGEBA/DDS. The FTIR spectra of DGEL/DDS and DGEBA/DDS at the maximum decomposition rate are exhibited in the Fig. 11b. All the absorption peak intensities for the two samples have been normalized. The similar gas volatiles decomposed from DGEL/DDS and DGEBA/DDS are detected, such as aromatic alcohols (3655–3652 $cm^{-1}$), hydrocarbons (2973 $cm^{-1}$), $CO_2$ (2362–2307

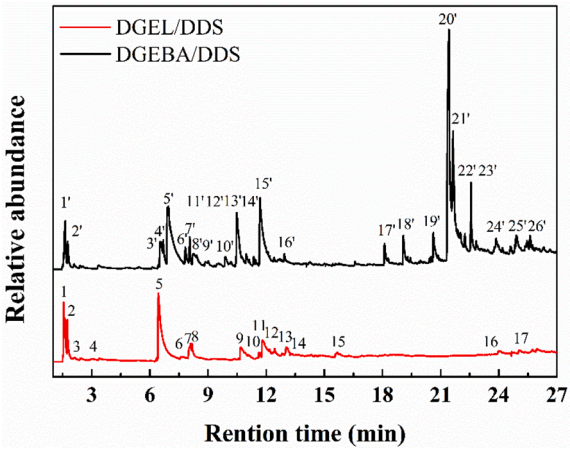


**Fig. 12.** Total ion chromatograms of Py-GC/MS for DGEL/DDS and DGEBA/DDS.

$cm^{-1}$), CO (2182 $cm^{-1}$), carbonyl compounds (1736–1733 $cm^{-1}$), aromatic compounds (1597–1506 $cm^{-1}$), $SO_2$ (1341–1342 $cm^{-1}$), Ar-O structure (1256 $cm^{-1}$) and aliphatic ethers (1175–1160 $cm^{-1}$) [66].

The release of aliphatic ethers, Ar-O structure, aromatic compounds, hydrocarbons and aromatic alcohols from DGEL/DDS during thermal decomposition are much lower than that from DGEBA/DDS (see Fig. 11c–g), indicating that most of these decomposed compounds are immobilized in the condensed phase. The thermal decomposition of DGEL/DDS also leads to the formation of carbonyl compounds (Fig. 11h). It is attributed to the destruction of four-membered ring formed during the intermolecular cross-linking reaction via C═C in benzopyrone ring that induces the generation of carbonyl-based volatiles (see Fig. S3). From the TGA-FTIR results, it can be implied that lots of aromatic structures are involved in carbonization reaction, which leads to the formation of stable char residues that efficiently inhibit the release of flammable gas volatiles.

To clearly understand the pyrolysis products, DGEL/DDS and DGEBA/DDS were measured by means of Py-GC/MS. The thermal decomposition route was inferred by studying the pyrolysis products at 500 °C. The total ion chromatograms of the sample are shown in Fig. 12. The detailed information of molecular weight corresponding to the chemical structure is summarized in Table S2 and Table S3. In the pyrolysis of DGEBA/DDS, the decomposition of BPA fragments lead to the release of acetaldehyde (peak 1′), phenol (peak 5′), 4-isopropylphenol (peak 11′), 4-isopropenylphenol (peak 15′), phenol, 4,4′-(1-methylethylidene) bis- (peak 20′), 3,4′-isopropylidenediphenol (peak 21′). The

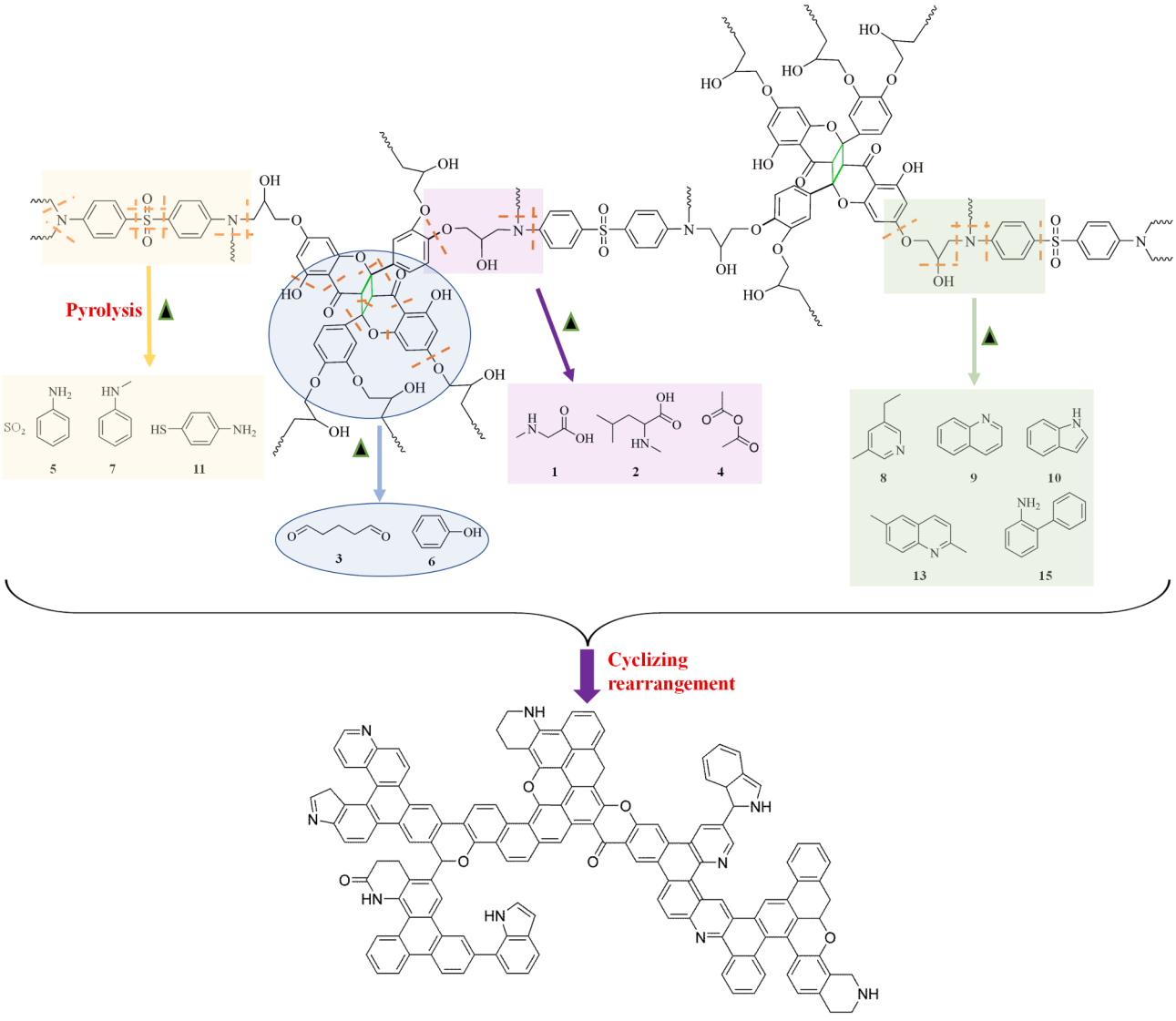


**Scheme 2.** The illustration of thermal decomposition and flame retardant mechanism for DGEL/DDS.

degradation of 4, 4-diaminodiphenyl sulfone segments results in the generation of aniline (peak 3′), N-methylaniline (peak 6′), N,N-dimethylaniline (peak 7′) and the other compounds. The results show that the main structure of DGEBA/DDS is destroyed during the pyrolysis, and lots of aromatic compounds with low molecular weight are released into the gas phase leading to a low char yield (Fig. S5).

Different from the pyrolysis of DGEBA/DDS, sarcosine (peak 1), N-methyl-L-leucine and aniline (peak 5) are primarily produced in the thermal decomposition of DGEL/DDS. The aromatic compounds, such as aniline (peak 5), N-methylaniline (peak 7) and 4-aminothiophenol (peak 11) are produced by the cleavage of 4, 4-diaminodiphenyl sulfone segment in DGEL/DDS. With the increase of temperature, benzopyrone ring structure in DGEL starts decomposition leading to the generation of glutaraldehyde (peak 3) and phenol (peak 6). It is worth noting that the intensity of phenol for DGEL/DDS is much lower than that for DGEBA/DDS (peak 5′). It suggests that most of the phenols decomposed from DGEL/DDS are involved in the cyclizing rearrangement with aniline (peak 5), 3-ethyl-5-methyl-pyridine (peak 8), quinoline (peak 9), indole (peak 10), 2,6-dimethylquinoline (peak 13) and other compounds, which leads to the formation of char residues (Scheme 2). It means that large amount of flammable decomposed products are immobilized in carbonized solids, thus reducing the emission of combustible volatiles. In consequence, the heat release and smoke productions are significantly decreased. Combined with the condensed-phase characterization of SEM and Raman, it can be concluded that DGEL/DDS shows more significant carbonization ability via rapid cyclization under high temperature compared to DGEBA/DDS. In addition, the char residues for DGEL/DDS are mechanically and thermally stable which can efficiently block the transfer of heat and flammable gas. It is beneficial for the protection of the internal resin matrix from further degradation leading to the reduction of flammability of the resin.

## 4. Conclusions

In this work, a novel fully bio-based epoxy monomer (DGEL) was synthesized by one-step method and high performance epoxy resin was obtained after curing with DDS. The $T_g$ of DGEL/DDS was 314.4 °C, indicating the outstanding heat resistance. The tensile strength of DGEL/DDS was 69.2 MPa, higher than that of DGEBA/DDS (57.2 MPa). Furthermore, DGEL/DDS showed excellent charring ability with the char yield of 44.0 wt% at 700 °C in $N_2$, much higher than that of DGEBA/DDS (11.6 wt%). MCC results demonstrated that DGEL/DDS possessed an extremely low PHRR of 107.5 W/g. DGEL/DDS achieved the V-0 rating of the UL-94 test with a notable high LOI (32.5%) suggesting the excellent flame retardant properties. Additionally, DGEL/DDS showed that the lower peak density of smoke (304.7) compared to that of DGEBA/DDS (660.7), indicating the reduced toxicity hazards. In summary, luteolin-based epoxy resins exhibited exceptional heat resistance, mechanical and fire retarded properties that have great potential for industrial and domestic applications.

## Declaration of Competing Interest

The authors declare that they have no known competing financial interests or personal relationships that could have appeared to influence the work reported in this paper.

## Acknowledgements

This work was co-financed by Anhui Provincial Natural Science Foundation for Distinguished Young Scholar (2008085J26), National Natural Science Foundation of China (21702042), Anhui Provincial Key Technologies R&D Program (202004a05020044 and 1804a09020070).

## Appendix A. Supplementary data

Supplementary data to this article can be found online at https://doi.org/10.1016/j.cej.2021.131173.

## References

[1] F.-L. Jin, X. Li, S.-J. Park, Synthesis and application of epoxy resins: a review, J. Ind. Eng. Chem. 29 (2015) 1–11.
[2] E.R. Rad, H. Vahabi, A.R. de Anda, M.R. Saeb, S. Thomas, Bio-epoxy resins with inherent flame retardancy, Prog. Org. Coat. 135 (2019) 608–612.
[3] Y. Ma, H. Liu, J. Wu, L. Yuan, Y. Wang, X. Du, R. Wang, P.W. Marwa, P. Petlulu, X. Chen, H. Zhang, The adverse health effects of bisphenol A and related toxicity mechanisms, Environ. Res. 176 (2019), 108575.
[4] Y.Q. Huang, C.K. Wong, J.S. Zheng, H. Bouwman, R. Barra, B. Wahlstrom, L. Neretin, M.H. Wong, Bisphenol A (BPA) in China: a review of sources, environmental levels, and potential human health impacts, Environ. Int. 42 (2012) 91–99.
[5] D.D. Seachrist, K.W. Bonk, S.-M. Ho, G.S. Prins, A.M. Soto, R.A. Keri, A review of the carcinogenic potential of bisphenol A, Reprod. Toxicol. 59 (2016) 167–182.
[6] S.Y. Lee, H.U. Kim, T.U. Chae, J.S. Cho, J.W. Kim, J.H. Shin, D.I. Kim, Y.-S. Ko, W. D. Jang, Y.-S. Jang, A comprehensive metabolic map for production of bio-based chemicals, Nat. Catal. 2 (1) (2019) 18–33.
[7] R. Auvergne, S. Caillol, G. David, B. Boutevin, J.P. Pascault, Biobased thermosetting epoxy: present and future, Chem. Rev. 114 (2014) 1082–1115.
[8] C. Zhang, T.F. Garrison, S.A. Madbouly, M.R. Kessler, Recent advances in vegetable oil-based polymers and their composites, Prog. Polym. Sci. 71 (2017) 91–143.
[9] F. Mustata, N. Tudorachi, Synthesis and thermal characterization of some hardeners for epoxy resins based on castor oil and cyclic anhydrides, Ind. Crop. Prod. 159 (2021) 113087.
[10] J. Xin, M. Li, R. Li, M.P. Wolcott, J. Zhang, Green epoxy resin system based on lignin and tung oil and its application in epoxy asphalt, ACS Sustain. Chem. Eng. 4 (5) (2016) 2754–2761.
[11] C. Gioia, M. Colonna, A. Tagami, L. Medina, O. Sevastyanova, L.A. Berglund, M. Lawoko, Lignin-based epoxy resins: unravelling the relationship between structure and material properties, Biomacromolecules 21 (2020) 1920–1928.
[12] F. Ferdosian, Z. Yuan, M. Anderson, C. Xu, Synthesis and characterization of hydrolysis lignin-based epoxy resins, Ind. Crop. Prod. 91 (2016) 295–301.
[13] S. Ma, X. Liu, Y. Jiang, L. Fan, J. Feng, J. Zhu, Synthesis and properties of phosphorus-containing bio-based epoxy resin from itaconic acid, Sci. China-Chem. 57 (3) (2014) 379–388.
[14] Y. Tian, Q. Wang, J. Cheng, J. Zhang, A fully biomass based monomer from itaconic acid and eugenol to build degradable thermosets via thiol–ene click chemistry, Green Chem. 22 (3) (2020) 921–932.
[15] T.K.L. Nguyen, S. Livi, B.G. Soares, G.M.O. Barra, J.-F. Gérard, J. Duchet-Rumeau, Development of sustainable thermosets from cardanol-based epoxy prepolymer and ionic liquids, ACS Sustain. Chem. Eng. 5 (9) (2017) 8429–8438.
[16] Y. Ecochard, M. Decostanzi, C. Negrell, R. Sonnier, S. Caillol, Cardanol and eugenol based flame retardant epoxy monomers for thermostable networks, Molecules 24 (2019) 1818.
[17] A.-S. Mora, R. Tayouo, B. Boutevin, G. David, S. Caillol, Synthesis of biobased reactive hydroxyl amines by amination reaction of cardanol-based epoxy monomers, Eur. Polym. J. 118 (2019) 429–436.
[18] C. Aouf, H. Nouailhas, M. Fache, S. Caillol, B. Boutevin, H. Fulcrand, Multi-functionalization of gallic acid. Synthesis of a novel bio-based epoxy resin, Eur. Polym. J. 49 (6) (2013) 1185–1195.
[19] J. Wan, B. Gan, C. Li, J. Molina-Aldareguia, E.N. Kalali, X. Wang, D.-Y. Wang, A sustainable, eugenol-derived epoxy resin with high biobased content, modulus, hardness and low flammability: synthesis, curing kinetics and structure–property relationship, Chem. Eng. J. 284 (2016) 1080–1093.
[20] C.-H. Chen, S.-H. Tung, R.-J. Jeng, M.M. Abu-Omar, C.-H. Lin, A facile strategy to achieve fully bio-based epoxy thermosets from eugenol, Green Chem. 21 (16) (2019) 4475–4488.
[21] Y. Tao, L. Fang, M. Dai, C. Wang, J. Sun, Q. Fang, Sustainable alternative to bisphenol A epoxy resin: high-performance recyclable epoxy vitrimers derived from protocatechuic acid, Polym. Chem. 11 (2020) 4500–4506.
[22] X. Wang, W. Guo, L. Song, Y. Hu, Intrinsically flame retardant bio-based epoxy thermosets: a review, Compos. Part B-Eng. 179 (2019) 107487.
[23] Y. Qi, Z. Weng, K. Zhang, J. Wang, S. Zhang, C. Liu, X. Jian, Magnolol-based bio-epoxy resin with acceptable glass transition temperature, processability and flame retardancy, Chem. Eng. J. 387 (2020), 124115.
[24] Y. Qi, Z. Weng, Y. Kou, L. Song, J. Li, J. Wang, S. Zhang, C. Liu, X. Jian, Synthesize and introduce bio-based aromatic s-triazine in epoxy resin: enabling extremely high thermal stability, mechanical properties, and flame retardancy to achieve high-performance sustainable polymers, Chem. Eng. J. 406 (2021), 126881.
[25] W. Xie, S. Huang, D. Tang, S. Liu, J. Zhao, Biomass-derived schiff base compound enabled fire-safe epoxy thermoset with excellent mechanical properties and high glass transition temperature, Chem. Eng. J. 394 (2020), 123667.
[26] S. Jin, L. Qian, Y. Qiu, Y. Chen, F. Xin, High-efficiency flame retardant behavior of bi-DOPO compound with hydroxyl group on epoxy resin, Polym. Degrad. Stabil. 166 (2019) 344–352.
[27] P. Wang, F. Yang, L. Li, Z. Cai, Flame retardancy and mechanical properties of epoxy thermosets modified with a novel DOPO-based oligomer, Polym. Degrad. Stabil. 129 (2016) 156–167.

[28] M. Zhang, A. Buekens, X. Li, Brominated flame retardants and the formation of dioxins and furans in fires and combustion, J. Hazard. Mater. 304 (2016) 26–39.
[29] Y. Shi, B. Yu, Y. Zheng, J. Yang, Z. Duan, Y. Hu, Design of reduced graphene oxide decorated with DOPO-phosphanomidate for enhanced fire safety of epoxy resin, J. Colloid. Interface. Sci. 521 (2018) 160–171.
[30] J.L. Lyche, C. Rosseland, G. Berge, A. Polder, Human health risk associated with brominated flame-retardants (BFRs), Environ. Int. 74 (2015) 170–180.
[31] L. Deng, M. Shen, J. Yu, K. Wu, C. Ha, Preparation, characterization, and flame retardancy of novel rosin-based siloxane epoxy resins, Ind. Eng. Chem. Res. 51 (24) (2012) 8178–8184.
[32] R. Chen, K. Hu, H. Tang, J. Wang, F. Zhu, H. Zhou, A novel flame retardant derived from DOPO and piperazine and its application in epoxy resin: flame retardance, thermal stability and pyrolysis behavior, Polym. Degrad. Stabil. 166 (2019) 334–343.
[33] L. Abidin, M. Mujeeb, S.S. Imam, M. Aqil, D. Khurana, Enhanced transdermal delivery of luteolin via non-ionic surfactant-based vesicle: quality evaluation and anti-arthritic assessment, Drug. Deliv. 23 (2016) 1069–1074.
[34] J. Dai, Y. Peng, N.a. Teng, Y. Liu, C. Liu, X. Shen, S. Mahmud, J. Zhu, X. Liu, High-performing and fire-resistant biobased epoxy resin from renewable sources, ACS Sustain. Chem. Eng. 6 (6) (2018) 7589–7599.
[35] J. Dai, N. Teng, J. Liu, J. Feng, J. Zhu, X. Liu, Synthesis of bio-based fire-resistant epoxy without addition of flame retardant elements, Compos. Part B-Eng. 179 (2019), 107523.
[36] K.A. Ellzey, T. Ranganathan, J. Zilberman, E.B. Coughlin, R.J. Farris, T. Emrick, Deoxybenzoin-based polyarylates as halogen-free fire-resistant, Macromolecules 39 (2006) 3553–3558.
[37] M.W. Szyndler, J.C. Timmons, Z.H. Yang, A.J. Lesser, T. Emrick, Multifunctional deoxybenzoin-based epoxies: Synthesis, mechanical properties, and thermal evaluation, Polymer 55 (2014) 4441–4446.
[38] X. Shen, L. Cao, Y. Liu, J. Dai, X. Liu, J. Zhu, S. Du, How does the hydrogen bonding interaction influence the properties of polybenzoxazine? an experimental study combined with computer simulation, Macromolecules 51 (2018) 4782–4799.
[39] M. Jouyandeh, S.M.R. Paran, A. Jannesari, D. Puglia, M.R. Saeb, Protocol for nonisothermal cure analysis of thermoset composites, Prog. Org. Coat. 131 (2019) 333–339.
[40] M. Jouyandeh, S.M.R. Paran, A. Jannesari, M.R. Saeb, 'Cure Index' for thermoset composites, Prog. Org. Coat. 127 (2019) 429–434.
[41] S. Ma, X. Liu, Y. Jiang, Z. Tang, C. Zhang, J. Zhu, Bio-based epoxy resin from itaconic acid and its thermosets cured with anhydride and comonomers, Green Chem. 15 (1) (2013) 245–254.
[42] M.G. Mohamed, K.-C. Hsu, S.-W. Kuo, Bifunctional polybenzoxazine nanocomposites containing photo-crosslinkable coumarin units and pyrene units capable of dispersing single-walled carbon nanotubes, Polym. Chem. 6 (13) (2015) 2423–2433.
[43] X. Xu, S. Ma, J. Wu, J. Yang, B. Wang, S. Wang, Q. Li, J. Feng, S. You, J. Zhu, High-performance, command-degradable, antibacterial Schiff base epoxy thermosets: synthesis and properties, J. Mater. Chem. A 7 (25) (2019) 15420–15431.
[44] T. Liu, L. Zhang, R. Chen, L. Wang, B. Han, Y. Meng, X. Li, Nitrogen-free tetrafunctional epoxy and its dds-cured high-performance matrix for aerospace applications, Ind. Eng. Chem. Res. 56 (27) (2017) 7708–7719.
[45] J. Deng, X. Liu, C. Li, Y. Jiang, J. Zhu, Synthesis and properties of a bio-based epoxy resin from 2,5-furandicarboxylic acid (FDCA), RSC Adv. 5 (21) (2015) 15930–15939.
[46] J.-T. Miao, L.i. Yuan, Q. Guan, G. Liang, A. Gu, Biobased heat resistant epoxy resin with extremely high biomass content from 2,5-furandicarboxylic acid and eugenol, ACS Sustain. Chem. Eng. 5 (8) (2017) 7003–7011.
[47] E.D. Hernandez, A.W. Bassett, J.M. Sadler, J.J. La Scala, J.F. Stanzione, Synthesis and characterization of bio-based epoxy resins derived from vanillyl alcohol, ACS Sustain. Chem. Eng. 4 (8) (2016) 4328–4339.
[48] W. Xie, D. Tang, S. Liu, J. Zhao, Facile synthesis of bio-based phosphorus-containing epoxy resins with excellent flame resistance, Polym Test. 86 (2020), 106466.
[49] J. Liu, Z. He, G. Wu, X. Zhang, C. Zhao, C. Lei, Synthesis of a novel nonflammable eugenol-based phosphazene epoxy resin with unique burned intumescent char, Chem. Eng. J. 390 (2020), 124620.
[50] I. Faye, M. Decostanzi, Y. Ecochard, S. Caillol, Eugenol bio-based epoxy thermosets: from cloves to applied materials, Green Chem. 19 (2017) 5236–5242.
[51] A.-S. Mora, R. Tayouo, B. Boutevin, G. David, S. Caillol, Vanillin-derived amines for bio-based thermosets, Green Chem. 20 (17) (2018) 4075–4084.
[52] J. Wan, J. Zhao, B. Gan, C. Li, J. Molina-Aldareguia, Y. Zhao, Y.-T. Pan, D.-Y. Wang, Ultrastiff biobased epoxy resin with high tg and low permittivity: from synthesis to properties, ACS Sustain. Chem. Eng. 4 (5) (2016) 2869–2880.
[53] J. Wan, B. Gan, C. Li, J. Molina-Aldareguia, Z. Li, X. Wang, D.-Y. Wang, A novel biobased epoxy resin with high mechanical stiffness and low flammability: synthesis, characterization and properties, J. Mater. Chem. A 3 (2015) 21907–21921.
[54] M. Shibata, T. Ohkita, Fully biobased epoxy resin systems composed of a vanillin-derived epoxy resin and renewable phenolic hardeners, Eur. Polym. J. 92 (2017) 165–173.
[55] X. Ma, W. Guo, Z. Xu, S. Chen, J. Cheng, J. Zhang, M. Miao, D. Zhang, Synthesis of degradable hyperbranched epoxy resins with high tensile, elongation, modulus and low-temperature resistance, Compos. Part B-Eng. 192 (2020), 108005.
[56] W. Yang, Y. Hu, Q. Tai, H. Lu, L. Song, R.K.K. Yuen, Fire and mechanical performance of nanoclay reinforced glass-fiber/PBT composites containing aluminum hypophosphite particles, Compos. Part A-Appl. Sci. Manuf. 42 (7) (2011) 794–800.
[57] R.E. Lyon, R.N. Walters, S.I. Stoliarov, Screening flame retardants for plastics using microscale combustion calorimetry, Prog. Polym. Sci. 47 (2007) 1501.
[58] R.N. Walters, N. Safronava, R.E. Lyon, A microscale combustion calorimeter study of gas phase combustion of polymers, Combust. Flame 162 (3) (2015) 855–863.
[59] M.-E. Li, S.-X. Wang, L.-X. Han, W.-J. Yuan, J.-B. Cheng, A.-N. Zhang, H.-B. Zhao, Y.-Z. Wang, Hierarchically porous SiO2/polyurethane foam composites towards excellent thermal insulating, flame-retardant and smoke-suppressant performances, J. Hazard. Mater. 375 (2019) 61–69.
[60] Y.-Y. Yen, H.-T. Wang, W.-J. Guo, Synergistic flame retardant effect of metal hydroxide and nanoclay in EVA composites, Polym. Degrad. Stabil. 97 (6) (2012) 863–869.
[61] B. Yu, B. Tawiah, L.-Q. Wang, A.C. Yin Yuen, Z.-C. Zhang, L.-L. Shen, B.o. Lin, B. Fei, W. Yang, A.o. Li, S.-E. Zhu, E.-Z. Hu, H.-D. Lu, G.H. Yeoh, Interface decoration of exfoliated MXene ultra-thin nanosheets for fire and smoke suppressions of thermoplastic polyurethane elastomer, J. Hazard. Mater. 374 (2019) 110–119.
[62] B. Yuan, Y. Hu, X. Chen, Y. Shi, Y. Niu, Y. Zhang, S. He, H. Dai, Dual modification of graphene by polymeric flame retardant and Ni(OH) 2 nanosheets for improving flame retardancy of polypropylene, Compos. Part A-Appl. Sci. Manuf. 100 (2017) 106–117.
[63] J.-N. Wu, L. Chen, T. Fu, H.-B. Zhao, D.-M. Guo, X.-L. Wang, Y.-Z. Wang, New application for aromatic schiff base: high efficient flame-retardant and anti-dripping action for polyesters, Chem. Eng. J. 336 (2018) 622–632.
[64] W. Yang, B. Tawiah, C. Yu, Y.-F. Qian, L.-L. Wang, A.-Y. Yuen, S.-E. Zhu, E.-Z. Hu, T.-Y. Chen, B. Yu, H.-D. Lu, G.H. Yeoh, X. Wang, L. Song, Y. Hu, Manufacturing, mechanical and flame retardant properties of poly(lactic acid) biocomposites based on calcium magnesium phytate and carbon nanotubes, Compos. Part A-Appl. Sci. Manuf. 110 (2018) 227–236.
[65] X. Wang, W. Xing, X. Feng, B. Yu, L. Song, Y. Hu, Functionalization of graphene with grafted polyphosphamide for flame retardant epoxy composites: synthesis, flammability and mechanism, Polym. Chem. 5 (2014) 1145–1154.
[66] W.-J. Liang, B. Zhao, P.-H. Zhao, C.-Y. Zhang, Y.-Q. Liu, Bisphenol-S bridged penta (anilino)cyclotriphosphazene and its application in epoxy resins: synthesis, thermal degradation, and flame retardancy, Polym. Degrad. Stabil. 135 (2017) 140–151.